SIMULTANEOUS DETERMINATION OF AEROSOL SIZE DISTRIBUTION AND REFRACTIVE INDEX AND SURFACE ALBEDO FROM RADIANCE——PART II: APPLICATION

Qiu Jinhuan (邱金桓), *Sun Jinhui* (孙金辉), *Xia Qilin* (夏其林), *Zhang Jinding* (张金定) and *Zhou Xiuji* (周秀骥)

Institute of Atmospheric Physics, Academia Sinica, Beijing

Received November 30, 1984

ABSTRACT

This paper presents and analyzes experimental results in simultaneous determination of atmospheric columnar aerosol size distribution, refractive index and surface albedo by use of the radiance data in almucantar measured by a radiometer. 32 groups of data measured in Beijing during winter show that the imaginary part of refractive index for 0.6943 μm wavelength ranges from 0.022 to 0.079 with a mean of 0.0527. The mean real part and surface albedo are 1.537 and 0.287, respectively. The imaginary part was found to be less in autumn than that in winter, especially after raining. For 0.399 μm and 0.6943 μm wavelengths, the mean surface albedos are 0.101 and 0.222, and the mean imaginary parts are 0.0241 and 0.0129, respectively.

I. INTRODUCTION

In our theoretical analysis[1], we have studied the principle of simultaneous determination of atmospheric aerosol size distribution (ASD), its refractive index (RI) and surface albedo (SA), and presented a set of reasonable inversion channels. This paper will present and analyze our experiment results.

II. EXPERIMENTS

A radiometer with the view angle of 3 mrad and two narrow-band filters centered at 0.399 μm and 0.6943 μm wavelengths was used to measure sky radiance in almucantar. It took about three minutes to measure a set of radiance data in azimuth angle ranging from 1° to 180°. Long method was used to determine atmospheric columnar optical depth. Experiments were made on the top of the main building of our institute situated in the north suburb of Beijing from December 1983 to October 1984.

52 groups of data under cloudless conditions were obtained. Shown in Fig. 1 are two groups of radiance normalized to that for scattering angle of 10°, which represent nearly simultaneous observations at two wavelengths. At larger azimuth angles the radiance curve at 0.399 μm is much smoother than that at 0.6943 μm because the atmospheric scattering phase function in shorter wavelength region largely depends upon the molecular phase function which is comparatively smooth at larger scattering angles. However, the two curves are approximately coincident in aureole region of azimuth angle ϕ less than 20°, where the sky radiance mainly depends on aerosol scattering.

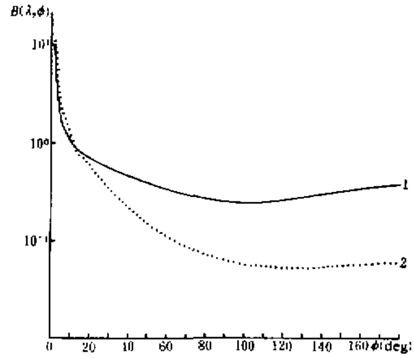

Fig. 1. Normalized radiance $B(\lambda,\phi)$ in almucantar on 19 Oct. 1984.
Curves 1 for 0836 LST, λ=0.399 μm; and 2 for 0904 LST, λ=0.6943 μm.

III. EXPERIMENTAL RESULTS AND DISCUSSIONS

The atmospheric columnar ASD in Beijing was inferred from aerosol volume scattering function with $1°\lesssim\theta\lesssim30°$ which was determined from measured sky radiance data by an approximate expression of radiance in almucantar presented in Part I of this paper[1]. Nonlinear regression method was used for retrieving the distribution with the following two-slope distribution as regressive function:

$$n(r)=c[1+(r/r_B)^{\nu_1}]/[1+(r/r_A)^{\nu_2}]. \quad (1)$$

The real and imaginary parts of aerosol RI were retrieved from the aerosol phase function near 10° and its weighted phase function near 40°. Mesh scanning method was

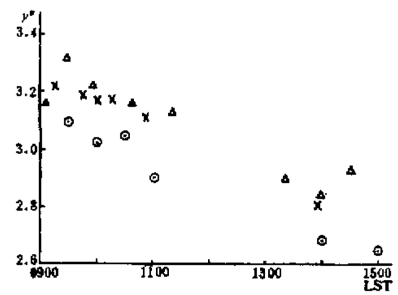

Fig. 2. Regressed Junge distribution parameters ν^*.
△ 8 Dec. 1983; X 15 Dec. 1983; ⊙ 12 Jan. 1984.

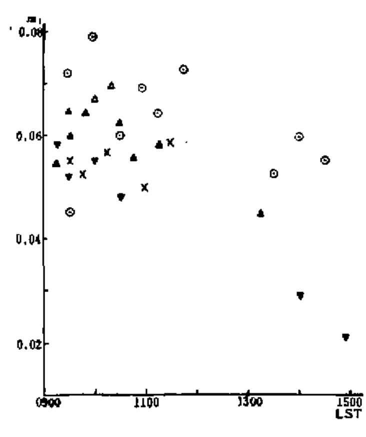

Fig. 3. Retrieved imaginary part at λ= 0.6943μm.
⊙ 8 Dec. 1983; △ 15 Dec. 1983; × 17 Dec. 1983; • 10 Jan. 1984, ▼ 12 Jan. 1984; ▲ 13 Jan. 1984.

applied for retrieving the imaginary part with the mesh values of 0, 0.005, 0.01, 0.015, 0.02, 0.03, 0.04, 0.05, 0.06, 0.08 and 0.1. The weighted phase function value between two meshes was determined by parabolic interpolation. Our observation data were obtained in the condition of solar zenith angle θ_0 larger than 40°. The radiances at 90° and 80° were used for inferring SA for solar zenith angles >45° and 40°—45°, respectively. An algorithm of joint determination of ASD, RI and SA was detailed in our theoretical study[1].

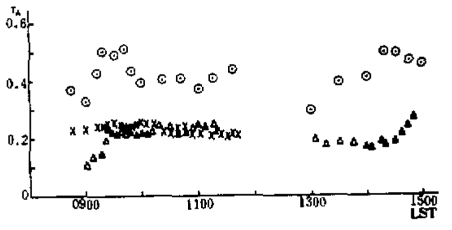

Fig. 4. Daily variation of aerosol optical depth at 0.6943 μm for some days of Dec. 1983. ⊙ 8th; △ 12th; × 17th.

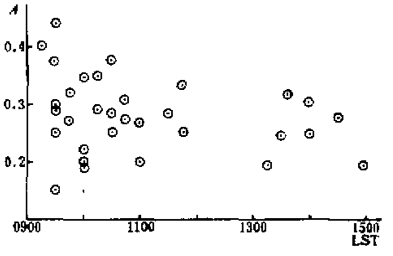

Fig. 5. Surface albedo at λ=0.6943 μm from 8 Dec. 1983 to 13 Jan. 1984.

Table 1. Inversion Results of RI and SA at λ=0.6943 μm

Date	$\bar{\tau}_A$	m_R	m_I	$\bar{A}$
8 Dec. 1983	0.421±0.120	1.57±0.06	0.067±0.014	0.26±0.07
15	0.258±0.094	1.53±0.05	0.060±0.016	0.30±0.11
17	0.234±0.045	1.55±0.03	0.055±0.006	0.25±0.05
10 Jan.1984	0.212±0.039	1.53±0.03	0.042±0.003	0.34±0.13
12	0.261±0.072	1.55±0.06	0.045±0.021	0.33±0.10
13	0.413±0.085	1.52±0.04	0.058±0.009	0.28±0.07
Average		1.547	0.0572	0.287
Standard Deviation		0.035	0.017	0.065
Variation Range		1.51—1.61	0.022—0.079	0.15—0.43

Table 2. Inversion Results of RI and SA at λ=0.6943 μm in Oct. 1984

Time (LST)	τ_A	m_R	m_I	A
0943, 6th	0.452	1.53	0.0188	0.141
1001, 6th	0.380	1.49	0.0139	0.248
0854, 12th*	0.078	1.50	0.0089	0.270
0904, 19th*	0.148	1.46	0.0122	0.203
0916, 19th*	0.153	1.49	0.0108	0.249
Average		1.494	0.0129	0.222

* First day after raining

Table 3. *Inversion Results of RI and SA at* $\lambda=0.399\,\mu m$

Time (LST)	τ_A	m_R	m_I	A
1345, 12 Oct.*	0.124	1.46	0.0161	0.142
1420,	0.202	1.49	0.0133	0.094
0825, 13 Oct.	0.640	1.52	0.0209	−0.096
0915,	0.652	1.48	0.0235	0.103
1020,	0.649	1.49	0.0271	0.043
1108,	0.662	1.52	0.0320	0.087
1323,	0.577	1.54	0.0196	−0.062
1428,	0.666	1.51	0.0224	0.122
1524,	0.645	1.47	0.0190	0.301
0921, 16 Oct.	0.342	1.54	0.0354	0.270
1423,	0.390	1.50	0.0291	0.060
0834, 17 Oct.	0.287	1.56	0.0315	−0.01
0929,	0.325	1.54	0.0380	0.260
1455,	0.402	1.51	0.0267	0.09
0828, 19 Oct.	0.312	1.48	0.0075	0.14
Average		1.507	0.0241	0.101
Standard Deviation		0.029	0.0081	0.112

* First day after raining

Tables 1—5 and Figs. 2—6 show some of the experimental results.

(1) *Atmospheric columnar ASD*

Junge distribution parameters ν^* regressed for winter observation data obtained from 8 Dec. 1983 to 13 Jan. 1984 vary between 2.6 and 3.3. As shown in Fig. 2, ν^* usually decreases from the morning to the afternoon, implying that the proportion of large particulates in the ASD gets larger. Many authors have observed similar phenomena[3,4].

The mean two–slope distribution regressed from all 52 groups of observation data is

$$n(r)=1.88\times10^{13}[1+(r/1.2)^{0.8}]/[1+(r/0.03)^{4.2}].$$

Two–slope distribution is usually more fit to observation data than Junge distribution.

(2) *Aerosol RI*

Fig. 3 shows the inferred imaginary part of RI at 0.6943 μm from 32 groups of observations in winter, and Table 1 shows the daily–mean values of aerosol optical depth, whose imaginary and real parts of RI and SA are marked by $\bar{\tau}_A$, $\bar{m}_R$, $\bar{m}_I$ and $\bar{A}$, respectively. Line 8 in Table 1 gives the "average " value obtained from 32 groups of inversion results.

From Fig. 3 and Table 1 we can see the following:

(A) The imaginary part of RI varies from 0.022 to 0.079 with a mean of 0.0572, and the real part is in the range of 1.51—1.63 with a mean of 1.547. Among our observations the aerosol optical depth on 8 Dec. 1983 is the largest and the corresponding imaginary part is larger with a maximum of 0.079. During 10—13 Jan. 1984 the imaginary part tended to increase with the increase of aerosol optical depth. Considering the fact pointed out by Wang Mingxing[5] that the major source of aerosol pollution in Beijing in winter is coal combustion, it is reasonable that the imaginary part increases with the increase of aerosol optical depth.

(B) The imaginary part of RI in the morning is generally larger than in the afternoon. Measurements made by Ander et al. show that the imaginary part of particulates in the range of $r>1$ μm is almost one order of magnitude less than that of particulates in the range of $0.1\leqslant r\leqslant 1$ μm. Our results show that from the morning to the afternoon the imaginary part gets smaller with the decrease of ν^*, i. e. with the increase of large particulate proportion, being consistent with Ander's results.

(C) Shown in Figs. 2—4 are the data obtained from 0930 to 1100 LST, 15 and 17 Dec. 1983 when the atmospheric condition was more stable. It can be seen that there are only a little changes in both aerosol optical depth and ASD, thus the deviation in the imaginary part is less than 0.003.

Table 2 shows 5 groups of imaginary part solutions at 0.6943 μm from data of Oct. 1984. The imaginary part varies from 0.0089 to 0.0188 with a mean of 0.0129. That is much less than the results in winter partly because three of experiments were carried out on the first day after raining.

Table 3 shows the inversion results at 0.399 μm from observations during 12—19 Oct. 1984. The mean real part of RI is 1.507; the imaginary part varies between 0.0075 and 0.0354 with a mean of 0.0241. On the first day after raining, or 12 or 19, Oct. both the aerosol optical depth and imaginary part were smaller; and the imaginary part in the morning is generally smaller than in the afternoon, consistent with the above-mentioned case at 0.6943 μm wavelength.

(3) *Surface albedo (SA)*

As shown in Table 1, the mean SA at 0.6943 μm in winter is 0.287 with a standard deviation of 0.065. In October, the mean SA at this wavelength is 0.222, being slightly less than that in winter (see Table 2). From Fig. 5 we can see that 32 SA solutions range from 0.15 to 0.44. Larger SA variation seems to be unrealistic in view of the impossibility of larger change of surface properties, associated with albedo in only a little more than one month. Furthermore, as shown in Table 3, the mean SA at 0.399 μm during 12—19, Oct 1984 is 0.101 with a rather large scatter, and even some unreasonable negative SAs are obtained. In our theoretical study[1], it was pointed out that as the total optical depth and the solar zenith angle are large, the sky radiance is insensitive to albedo. For 0.399 μm wavelength $\tau_m=0.349$, i. e. molecular optical depth is larger, so the sensitivity of radiance to albedo is weaker, especially in the case of larger optical depth and solar zenith angle. This situation can be exampled by the experiment at 0825 LST 13 Oct. 1984 for which $\theta_0=68.5°$ and $\tau_T=0.989$. Taking Junge distribution of $\nu^*=3$, $m=1.5-0.01i$ and $A=0.1$ we can find through radiative transfer calculation that as $A=0.2$, the variation of radiance at $\theta=90°$ in almucantar is less than 2.8%. Thus, if the observation error in the radiance is equal to -3% or 3%, the solution to SA is -0.12 or 0.32. It means that the accuracy in SA solution is low for large θ_0 and τ_T. In December and January of Beijing, the solar zenith angle is always larger than 60° and it can be found from Fig. 5 and Table 3 that as the total optical depth and solar zenith angle are larger, the deviation of SA solutions is quite significant. However, as will be mentioned, the mean SA solution seems to be reasonable.

(4) *Discussions*

Paltridge and Platt have pointed out that the imaginary part of atmospheric aerosol RI generally ranges from 0.005 to 0.02[7], but our results in winter in Beijing are in the range of 0.022—0.079, much larger than 0.005—0.02. In consideration of the atmospheric pollution situation in Beijing and in reference to some other authors' results, a larger imaginary part in winter is possible. Absorption in the visible region is mainly due to the presence of carbon and graphite particles. For typical carbonaceous aerosols the imaginary part can be up to 0.66. Many authors have obtained even larger imaginary part than ours in polluted industrialized areas or other partly polluted continental areas. Comparing the theoretical with measured ellipticities of light scatterd by turbid air, Eiden has inferred that the imaginary part of aerosol RI at Mainz lies in the range of 0.01 to 0.1[8]. Lin et al. have estimated the imaginary part of particulates of New York City to vary from 0.028 to 0.050 with a mean value of 0.040[9]. During the winter heating period in Beijing the carbon particle pollution caused by coal-combustion is very serious[5] and it results in a large imaginary part of particulates. The imaginary part of aerosol RI generally increases as the relative humidity of the air increases. The retrieved imaginary part in October, 1984 is much less than that in winter just because of the large relative humidity after raining and the less serious coal ash pollution.

Further study is devoted to analyzing the sensitivity of the imaginary part solution to the iterative initial values of both the real part and albedo. As shown in Table 4, as the first guess of the real part $m_R^{(0)}$ varies from 1.46 to 1.62, the deviation of the imaginary part inferred from observation data at 1030 LST 15 Dec. 1983 is less than 0.0054, but the difference of albedo can be up to 0.272. Table 5 shows that by use of the observations at 1323 LST 13 Oct. 1984, the imaginary part solution $m_I^{(1)}$ through the first iteration is 0.0217 in the case of $A^{(0)}=0.25$. And after the 5th iteration, although there is unreasonable negative albedo of -0.062, the imaginary part solution $m_I^{(5)}$only remains a difference of 0.00211 from $m_I^{(1)}$. This is consistent with the theoretical analysis. Besides, it is found that the imaginary part solution is less sensitive to the ASD than the real part and albedo solutions are.

In order to further analyze the reasonableness of our results, a comparison between measured radiance and computed one is illustrated in Fig. 6, in which the abscissa represents azimuth angle ϕ and the ordinate represents radiance $b(\lambda,\phi)$. Curve 1 shows the

Table 4. The Sensitivity of Imaginary Part and Albedo Solutions to the First Guess of Real Part for $\lambda=0.6943$ μm

$m_R^{(0)}$	1.46	1.48	1.50	1.52	1.54	1.56	1.58	1.6	1.62
m_I	0.0639	0.0636	0.0625	0.0614	0.0604	0.0597	0.0595	0.0590	0.0588
A	0.390	0.361	0.340	0.302	0.258	0.219	0.181	0.148	0.118

Table 5. The Variations of Imaginary Part and Albedo in Iterative Process for $\lambda=0.399$ μm

n	0	1	2	3	4	5
$m_I^{(n)}$		0.0217	0.0203	0.0199	0.0196	0.0196
$A^{(n)}$	0.25	0.0774	0.0059	−0.036	−0.061	−0.0602

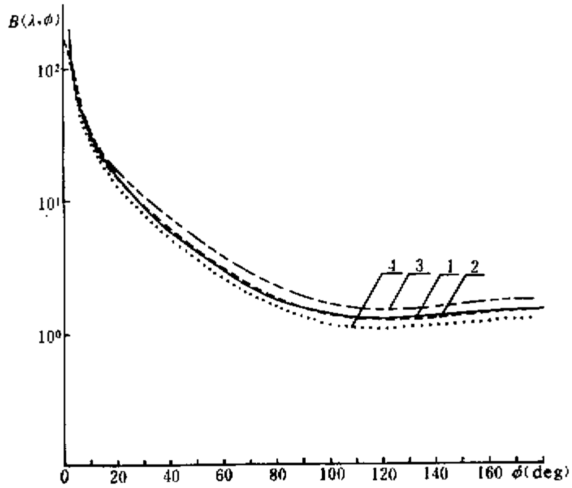

Fig. 6. A comparison between computed and measured radiances at 1456 LST 12, Jan. 1984 for $\lambda=0.6943$ μm.
Curves 1 for the measured radiance; 2, the computed, $m_I=0.022$; 3, the computed, $m_I=0.001$; and 4, the computed, $m_I=0.05$.

measured radiance from which the RI of $m=1.52-0.022i$, the SA of $A=0.31$ and the ASD of $n(r)=[1+(r/0.6)^{0.92}]/[1+(r/0.06)^{3.9}]$ were inferred. Curve 2 shows the radiance in almucantar calculated from the above retrieval data, which is closely coincident with the measured in the range of $4^0<\phi<180^0$. However, as $m_I=0.001$ is assumed instead of 0.022 and other parameters are the same as above, the calculated radiance is systematically larger than the measured. On the other hand, as $m_I=0.05$, the calculated radiance is systematically less. Thus, the moderate value $m_I=0.022$ is more fit to explain our observational data.

According to Kondratyev's study, SA is closely wavelength-dependent in general, and the albedo in ultraviolet region is down by a factor of 2 or 3 to that in visible region[10]. Weighted mean albedo at Tucson, Arizona inferred by King from diffuse-direct ratio data was found to be 0.279 for 0.5217—0.6708 μm wavelength range[11]. Our results show that in the October of Beijing, the mean SA is 0.222 at 0.6943 μm, about 2.2 times larger than that at 0.399 μm. Both SAs are larger than the data of corresponding wavelengths given by Kondratyev[10] for vegetation-covered surface. If there is no systematical error in measurements and the albedo averaged for several experiments is used, our method can be expected to provide reliable information on SA.

IV. CONCLUSION

From the view point of experiments, our method for the simultaneous determination of ASD, whose RI and SA from radiance data measured with a multiple-wavelength radiometer is more simple and economical, the primary experimental results being basically reasonable. Owing to the abundance of strongly-absorbing ash particles released by coal-combustion during the heating period in winter, the mean imaginary part of RI is found to be 0.0527 with a variation range of 0.022—0.079. Both real and imaginary parts are larger in winter than in autumn. Generally speaking, from the morning to the afternoon the ASD broadens and the imaginary part decreases. The albedo solution becomes more sensitive to the errors in measured sky radiance as total optical depth and solar zenith angle increase, resulting in the less accuracy in albedo solution. Our mean SA seems to be more suitable and it is basically consistent with Kondratyev's conclusion that the albedo at 0.6943 μm wavelength is a little more than twice of that at 0.399 μm.

In this paper, the spheric particle and the plane-parallel and homogeneous atmosphere are assumed. We will further study the effect of these assumptions on inferring RI and SA in the future.

REFERENCES

[1] Qiu Jinhuan and Zhou Xiuji, *Adv. Atmos. Sci.*, 3(1986), 162—171.
[2] Qiu Jinhuan, *Ibid.*, 3(1986), 1—9.
[3] Eiden, R., *Tellus*, 20(1968), 380—398.
[4] 邱金桓等, 大气科学, 7(1983), 380—398.
[5] 王明星, 科学探索, 3(1983), 13—20.
[6] Andre, K. et al., *J. Atmos. Sci.*, 38(1981), 141—155.
[7] Paltridge, G.W. and Platt, C.M.R., *Radiative Processes in Meteorology and Climatology*, Elesvier, 1976.
[8] Eiden, R., *Appl. Opt.*, 5(1966), 569—575.
[9] Lin, C.I. et al., *Appl. Opt.*, 12(1973), 1356—1363.
[10] Kondratyev, K.Y., *Radiation Characteristics of the Atmosphere and the Earth's Surface*, Amerind, New Delhi, 580 pp., 1973.
[11] King, M.D., *J. Atmos. Sci.*, 36(1979), 1072—1083.